Analyzing the Independent Effects of Paclitaxel and Carboplatin on BRCA-Mutant Ovarian Cancer Cells Under Hypoxia

By
Kruti Savani
Sc.M., Brown University

Thesis

Submitted in partial fulfillment of the requirements for the Degree of Master of Science in the Graduate Program of Biomedical Engineering at Brown University

PROVIDENCE, RHODE ISLAND

May 2026

AUTHORIZATION TO LEND AND REPRODUCE THE THESIS

As the sole author of this thesis, I authorize Brown University to lend it to other institutions for the purpose of scholarly research.

Date 04/29/26

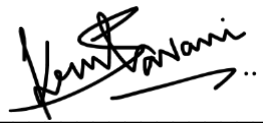

Kruti Savani, Author

I further authorize Brown University to reproduce this thesis by photocopying or other means, in total or in part, at the request of other institutions or individuals for the purpose of scholarly research.

Date 04/29/26

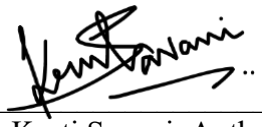

Kruti Savani, Author

This thesis by Kruti Savani is accepted in its present form by the Center for Biomedical Engineering as satisfying the thesis requirements for the degree of Master of Science

Date _____ Signature: _____
Dr. Michelle R. Dawson, Advisor

Date _____ Signature: _____
Dr. Edith Mathiowitz, Reader

Date _____ Signature: _____
Dr. Theresa Raimondo, Reader

Approved by the Graduate Council

Date _____ Signature: _____
Dr. Marissa Gray, Biomedical Engineering
Master's Program Director

Preface & Acknowledgments:

All work as presented in this thesis was conducted in the Center for Biomedical Engineering at Brown University in Providence, RI, United States. I, Kruti Savani, was responsible for formulating project ideas, conducting experiments, collecting data, analyzing results, and composing the thesis.

I am deeply grateful to everyone who supported me throughout this research journey. First and foremost, I would like to thank my research advisor, Dr. Michelle Dawson, for welcoming me into her lab and giving me the opportunity to contribute to such meaningful work. Her guidance, encouragement, and dedication to her students made this experience truly invaluable, and I am grateful for everything I have learned under her mentorship.

I would also like to extend my sincere thanks to my research mentor, Dr. Deepraj Ghosh, whose patience and expertise were instrumental in shaping this project. His willingness to answer my questions, troubleshoot experiments alongside me, and offer thoughtful direction at every stage of this work made an enormous difference. I am truly grateful for his time and commitment.

To all other members of the Dawson Lab, thank you for all additional help and valuable advice. Particularly, PhD candidates Basel White and Xingjian (Gavin) Lu, thank you for always being so willing to lend a helping hand. The patience and generosity you showed me throughout this experience is a true reflection of the incredible researchers and mentors you are becoming.

Lastly and most importantly, thank you to my family and friends for their support and motivating words.

Table of Contents

Abstract:

Abstract of Analyzing the Independent Effects of Paclitaxel and Carboplatin on BRCA-Mutant Ovarian Cancer Cells Under Hypoxia, *by Kruti Savani, Sc.M., Brown University, May 2026.*

Ovarian cancer carries a disproportionately high mortality rate relative to its incidence, largely due to late-stage diagnosis and the frequent development of resistance to standard chemotherapy. Among the most clinically significant contributors to poor prognosis are mutations in the BRCA1 and BRCA2 genes, which compromise homologous recombination repair and promote genomic instability. Despite the established clinical relevance of these mutations, how they shape cellular responses to chemotherapy and hypoxic stress remains incompletely understood.

This study investigated nuclear morphology and polyploid giant cancer cell (PGCC) formation in ID8 BRCA1 and ID8 BRCA2 mutant ovarian cancer cells under hypoxic and normoxic conditions, and examined the effect of paclitaxel and carboplatin treatment on these parameters. PGCCs are an understudied population of abnormally enlarged cancer cells with documented roles in chemoresistance and tumor repopulation following treatment. Results showed that hypoxia promoted nuclear enlargement and irregularity in both BRCA mutant cell lines, and that chemotherapeutic treatment dramatically amplified PGCC formation from a baseline of approximately 0.75-2.06% to as high as 63% regardless of oxygen conditions. DNA damage signaling was confirmed within PGCC nuclei through H2AX immunofluorescence staining. These findings suggest that standard chemotherapy may enrich for a resistant PGCC population in BRCA mutant ovarian cancer cells, with implications for understanding treatment resistance and developing more targeted therapeutic strategies.

Chapter 1: Introduction

Cancer is a broad group of diseases characterized by the uncontrolled proliferation of abnormal cells capable of invading surrounding tissues and distant organs.[1] All cancer cells share fundamental disruptions in the regulatory circuits governing normal cell proliferation and homeostasis, including the ability to sustain proliferative signaling, evade growth suppressors, activate invasion and metastasis, enable replicative immortality, induce angiogenesis, and resist cell death.[2] Subsequent research has recognized genomic instability as a critical enabling characteristic underlying these hallmarks, facilitating the mutational events that drive cancer progression.[3] Globally, cancer represents one of the foremost causes of morbidity and mortality, accounting for approximately one in six deaths worldwide, with an estimated 20 million new cases and 9.7 million deaths recorded in 2022 alone.[4,5] Among the many cancer types affecting women, gynecologic malignancies - those arising from the female reproductive organs - constitute a clinically significant and challenging subgroup, of which ovarian cancer carries a disproportionately high mortality burden relative to its incidence.[6]

Ovarian Cancer: Epidemiology and Clinical Challenges

Ovarian cancer is a rare but lethal malignancy that is frequently undetected in its early stages, contributing to its status as a leading cause of cancer-related mortality among women. In the United States, an estimated 20,890 new cases were projected to be diagnosed and approximately 12,730 deaths are likely to be attributed to ovarian cancer in 2025 alone.[6] While ranking as the eleventh most common cancer among women, ovarian cancer is the fifth leading cause of cancer-related death in this population, underscoring its lethality relative to incidence.[7] The overall five-year survival rate for ovarian cancer patients is approximately 47%; however, this figure drops

dramatically to 29.2% for high-grade serous ovarian carcinoma (HGSOC), the most common and lethal histological subtype.[8,9]

Epithelial ovarian cancer is further classified into five histological subtypes: HGSOC, low-grade serous carcinoma (LGSC), mucinous carcinoma (MC), endometrioid carcinoma (EC), and clear cell carcinoma (CCC), each distinguished by unique genetic and phenotypic characteristics.[10] HGSOC is defined by near-universal mutations in the *TP53* tumor suppressor gene, which is found in nearly all HGSOC tumors and is considered a driver of its development.[11] Germline mutations in *BRCA1* and *BRCA2* are found in 20–22% of HGSOC tumors and are among the most clinically important molecular features of this disease, as they impair homologous recombination-based DNA repair and increase genomic instability.[12] Critically, approximately 80% of HGSOC cases are diagnosed at late-stage or metastatic conditions, at which point curative intervention becomes significantly more difficult.[13] Despite the availability of chemotherapeutic treatments, HGSOC survival rates have not substantially improved over recent decades, with the majority of patients experiencing disease recurrence within three to five years of first-line therapy.[14] This pattern of late diagnosis, high relapse rates, and the development of chemotherapy resistance represents the central clinical challenge in ovarian cancer management.

Current Treatment Strategies for Ovarian Cancer

The standard of care for ovarian cancer combines cytoreductive surgery with systemic chemotherapy, with the extent of surgical debulking recognized as an important determinant of survival outcomes.[15] Chemotherapy represents the primary therapeutic approach, functioning by disrupting cellular proliferation. Among chemotherapeutic agents, paclitaxel and platinum-based

drugs - including carboplatin - are the most widely employed in ovarian cancer management, typically used in combination to suppress tumor growth.[15,16]

Carboplatin is a platinum-based compound that exerts its cytotoxic effect through the formation of intrastrand and interstrand DNA crosslinks, which structurally alter the DNA, stall replication forks, prevent DNA synthesis, and ultimately trigger cell cycle arrest and apoptosis in rapidly dividing cells.[17,18] Paclitaxel, a taxane-class chemotherapeutic agent, operates through a mechanistically distinct pathway: it binds to and stabilizes polymerized microtubules, thereby preventing their depolymerization, arresting cells in the G2/M phase of the cell cycle, and inducing apoptosis.[19] The complementary mechanisms of these two agents - one targeting DNA integrity, the other targeting mitotic machinery - provide the biological rationale for their use in combination, enabling simultaneous disruption of multiple critical cell processes.[15,16]

Chemotherapy Resistance in Ovarian Cancer

Despite the initial efficacy of paclitaxel and carboplatin combination therapy, the frequent development of resistance, particularly to platinum-based agents, remains a major obstacle in ovarian cancer management.[14] The mechanisms underlying resistance are multifactorial, encompassing alterations in drug influx and efflux, enhanced DNA repair capacity, evasion of apoptotic signaling, and reversion of *BRCA1/2* mutations.[20,21] Mutations in *BRCA1/2* confer sensitivity to DNA-damaging agents such as platinum chemotherapy precisely because these cells already have a compromised homologous recombination repair pathway; however, reversion mutations or alternative repair pathway activation can restore resistance over time.[20] Critically, the DNA damage response (DDR) deficiency caused by *TP53* and *BRCA1/2* mutations may alter sensitivity to therapy and thereby affect the overall progression of the disease.[21]

Beyond intrinsic cellular mechanisms, the tumor microenvironment (TME) plays an increasingly recognized role in modulating chemosensitivity, as the physical and biochemical conditions surrounding tumor cells can profoundly influence drug delivery and cellular response.[22] The TME is principally composed of the extracellular matrix (ECM) and stromal cells - including immune cells, cancer-associated fibroblasts (CAFs), adipocytes, and endothelial cells - all of which interact dynamically to promote or suppress tumor growth and treatment response.[22,23] Fibroblasts within the TME are of particular relevance; upon activation into CAFs by inflammatory cytokines such as TGF-β, they promote tumor cell proliferation, migration, ECM remodeling, and epithelial-mesenchymal transition, collectively signifying poor prognosis.[24]

Hypoxia in the TME

A defining feature of solid tumors, including ovarian cancer, is the development of hypoxia - a state of insufficient oxygen supply arising when rapidly proliferating tumor cells outgrow their existing vasculature.[25] Hypoxia activates a transcriptional program primarily orchestrated by hypoxia-inducible factor-1α (HIF-1α), which promotes tumor cell survival, angiogenesis, metabolic reprogramming, and resistance to apoptosis, collectively enabling tumor cells to thrive under oxygen-deprived conditions.[25,26] Ovarian cancers are highly hypoxia-dependent, with ascites further worsening oxygen accessibility within the peritoneal tumor environment, and approximately three-quarters of patients are diagnosed at Stage III or IV with disseminated disease in which hypoxia is a prominent feature.[27]

Hypoxia has been demonstrated to significantly alter cellular responses to chemotherapy, contributing to both intrinsic and acquired drug resistance.[26,27] Malformed and poorly permeable tumor vasculature impedes uniform drug delivery to tumor cells, while the reduction in reactive

oxygen species (ROS) under hypoxic conditions diminishes the cytotoxic activity of platinum-based agents that partially depend on ROS generation for their mechanism of action.[25] Additionally, HIF-1α has been identified as an important target for improving cancer cell sensitivity to cisplatin and carboplatin, as its activation of the PI3K/AKT and MAPK/ERK pathways promotes cell survival and resistance.[27] Hypoxia thus represents a clinically significant microenvironmental condition that closely mimics the physiological state of the tumor and contributes meaningfully to therapeutic failure, providing a strong rationale for studying drug responses under hypoxic conditions.

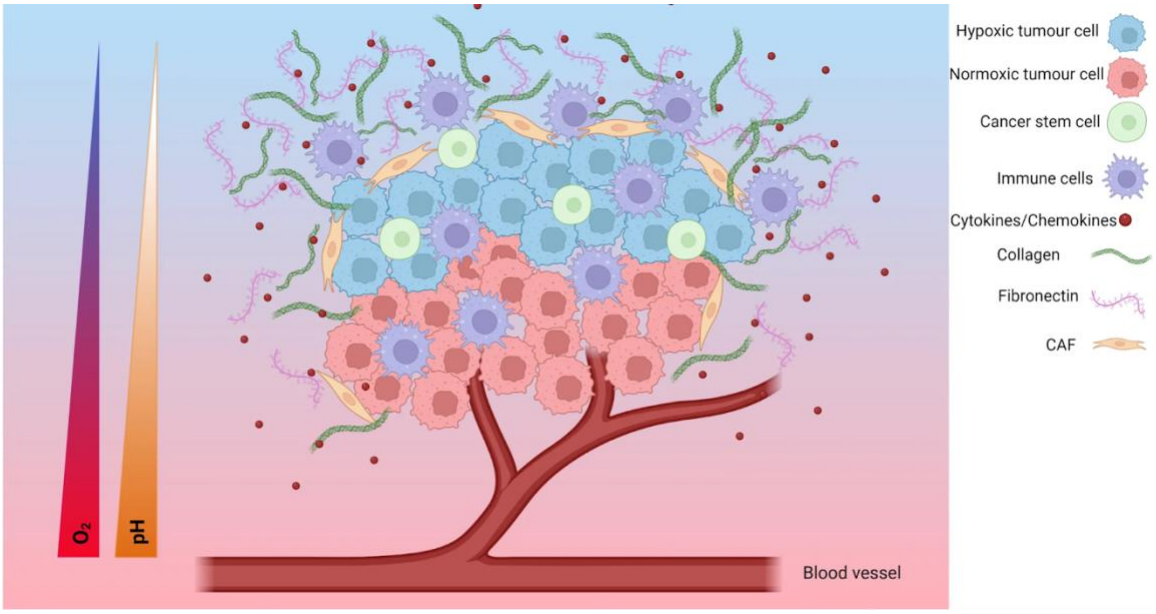

Figure 1. *The hypoxic tumor microenvironment, Bigos et al., Frontiers in Oncology, (2024).*

Polyploid Giant Cancer Cells (PGCCs)

Polyploid giant cancer cells (PGCCs) are a distinct subpopulation of tumor cells characterized by markedly enlarged cell size - approximately 3 to 10 times larger than normal cancer cells - and significantly elevated DNA content, reflected in enlarged or multiple nuclei.[28] PGCCs arise

through failures within the normal mitotic process or through overall genomic instability, and their formation can be triggered by a variety of cellular stresses, including hypoxia, chemotherapy, and radiation.[29] Three principal pathways have been identified for PGCC formation: endoreplication (endocycle), in which cells cycle between G and S phases without division, resulting in a large mononucleated cell with increased DNA content; endomitosis, in which the mitotic stage is entered but not completed; and cell fusion, in which two or more cells combine to form a single large cell independent of the cell cycle.[30,31]

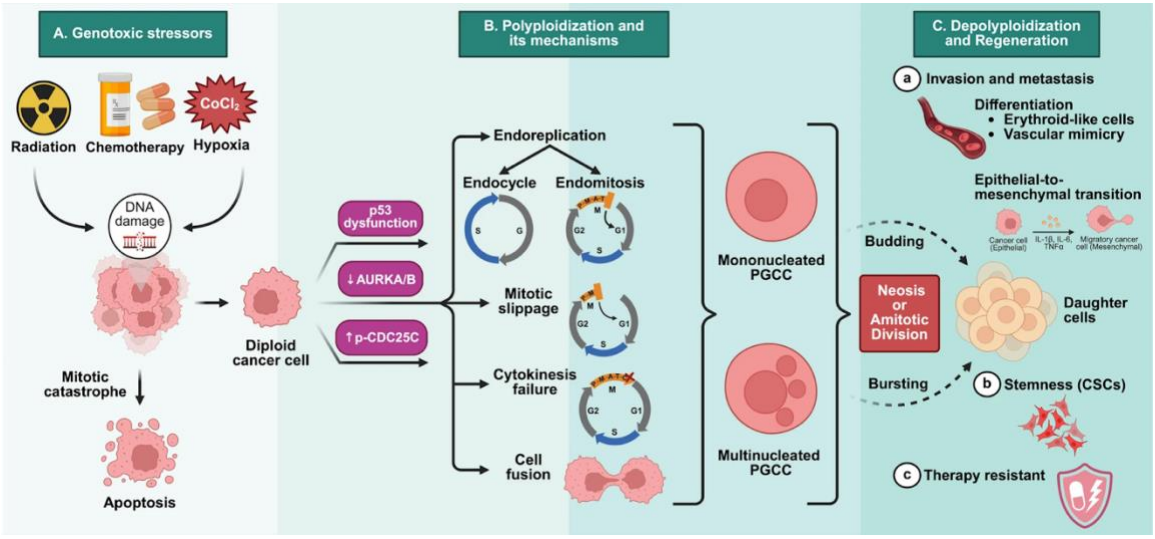

Figure 2. *Mechanisms of PGCC formation and their role in therapy resistance, Manickasamy et al. (2026).*

Although abnormal nuclear morphology has long been recognized as a feature that distinguishes cancer from benign tumors, PGCCs were historically considered senescent and incapable of division. However, emerging research has revealed that this subpopulation holds a crucial and active role in cancer progression and response to treatment.[32] PGCCs are frequently observed following exposure to chemotherapeutic stress and are capable of entering a dormant state in which they avoid cytotoxicity - as chemotherapeutics primarily target actively dividing cells - before re-

entering the cell cycle and dividing into daughter cells.[33] These daughter cells exhibit cancer stem cell characteristics, including the capacity for self-renewal and differentiation, and have been implicated in tumor repopulation after treatment.[29] PGCCs have been found to play a role in prognosis, survival, metastasis, and chemoresistance across multiple cancer types, including ovarian cancer, and represent an important contributor to intra-tumor heterogeneity.[33,34] Intra-tumor heterogeneity refers to the diversity of cells within the same tumor and the varying mechanisms by which subpopulations evade treatment; PGCCs, as an outlier population, may be overlooked in standard biopsy analyses, potentially leading to treatment decisions that fail to account for their invasive or resistant properties.[35]

Study Rationale and Research Objectives

Collectively, the challenges outlined above - late-stage diagnosis, high relapse rates, platinum resistance, hypoxia-driven microenvironmental adaptation, and the emergence of PGCCs - underscore the need for a more granular understanding of how ovarian cancer cells respond to chemotherapy under physiologically relevant conditions. The ID8 murine ovarian cancer cell line and its CRISPR/Cas9-derived *Trp53* and *Brca2* knockout derivatives provide a well-validated model system for studying hallmark mutation effects in the context of HGSOC biology, as these mutations recapitulate the most commonly observed genomic alterations in this disease.[36] Importantly, the absence of these genes has been shown to alter not only intracellular DDR signaling but also the composition and behavior of immune and stromal cells within the TME, further supporting the use of these cell lines for studying mutation-specific microenvironmental interactions.[36]

While prior work using these cell lines has characterized PGCC formation and TME interactions with fibroblasts under standard culture conditions,[37] the independent effects of paclitaxel and carboplatin as single agents under hypoxic stress - a condition that closely mimics the physiological tumor environment - remain to be defined in the *BRCA1/2* mutant context. Understanding how specific genetic mutations shape therapeutic response under hypoxic conditions is essential for identifying mechanisms of resistance and potential targets for more precise therapeutic strategies. This study therefore examines the independent effects of paclitaxel and carboplatin on ID8 *BRCA1/2* mutant ovarian cancer cells under hypoxic conditions, with the aim of characterizing changes in growth, morphology, and recovery, and of elucidating how specific genetic mutations shape therapeutic response and interactions within the tumor microenvironment.

Chapter 2: Methods

Cell Culture

The cell lines used to model ovarian cancer were ID8-*Brca1*$^{-/-}$ and ID8-*Brca2*$^{-/-}$. The parental ID8 cell line was established to model ovarian cancer from C57BL/6 mice. However, this model is not truly representative of characteristic mutations in ovarian cancer, namely *BRCA1/2* (*Brca1/2* in mice). The cell line derivatives used in this study were created with gene editing technology to more accurately represent ovarian cancer biology. Both ovarian cancer cell types were cultured in DMEM (Corning) supplemented with 4% fetal bovine serum (FBS) (Bio-Techne), 1% penicillin streptomycin (PS) (Corning), and ITS (5 µg/mL insulin, 5 µg/mL transferrin, and 5 ng/mL sodium selenite). The ID8 cell lines used in this study were originally developed by Dr. Ian McNeish.

Fresh media was given every 48-72 hours until approximately 80% confluence was reached. Once confluent, cells were passaged by first washing with Dulbecco's Phosphate Buffered Saline (DPBS) (Corning) and detaching from tissue culture plates with 0.25% Trypsin-EDTA (Corning). The trypsin was neutralized with DMEM supplemented with 10% FBS and 1% PS. Cells were resuspended in their respective media and replated. All cells were incubated at 5% CO_2 and 37°C.

RNA Isolation and Quantitative Reverse Transcription Polymerase Chain Reaction (RT-qPCR)

TRIzol reagent was used to isolate RNA from cells according to the manufacturer's instructions. RNA concentration was measured using a spectrophotometer (Nanodrop 1000; Thermo Fisher Scientific). Genomic DNA (gDNA) was removed and cDNA synthesis was carried out with SYBR Green Master Mix (Bio-Rad) according to the manufacturer's instructions. 1 µg of RNA was used for PCR analysis. 18S and β-Actin were used as housekeeping genes to normalize expression of

the genes of interest, *Brca1* and *Brca2*. The quantification cycle (Cq) was measured for each sample, and the mean Cq for the housekeeping gene was subtracted from the mean Cq for the gene of interest to obtain a delta Cq value. Fold change was then calculated and normalized to the control sample.

Paclitaxel and Carboplatin Treatment

To prepare cells for therapeutic treatment, ID8-*Brca1*$^{-/-}$ and ID8-*Brca2*$^{-/-}$ cells were seeded in 24-well plates at either 50,000 or 1M cells per well depending on the experimental condition, as specified in the relevant figure legends. All treatment experiments were conducted under hypoxic/normoxic conditions (21% O_2, 5% CO_2, 37°C).

For paclitaxel (Cayman Chemical) treatment, each cell line was treated at a concentration of 500 nM with three technical replicates. For carboplatin (Cayman Chemical) treatment, each cell line was treated at two concentrations - 50 μM and 100 μM - with three technical replicates each.

Carboplatin is a platinum-based chemotherapeutic whose mechanism of action involves binding to DNA to form platinum-DNA adducts. These crosslinks physically distort the DNA structure, preventing DNA synthesis and ultimately inducing cell cycle arrest and apoptosis (Basu & Krishnamurthy, 2010). Paclitaxel acts through a distinct mechanism, stabilizing microtubules and thereby preventing the formation of the mitotic spindle, which halts the cell cycle at the G2/M phase and triggers apoptosis (Awosika et al., 2023).

For both drug treatments, cells were incubated with the drug for 72 hours. Following this treatment period, drug-containing media was removed, cells were washed with DPBS, and fresh complete media was added to allow for a 7-day recovery period. The recovery period was included to allow

for observation of post-treatment phenotypic changes, such as polyploid giant cancer cell (PGCC) formation or cellular regrowth, which may not be evident immediately after drug removal. After the recovery period, cells were fixed and stained for imaging as described in the Fixing and Immunostaining section.

Immunostaining

Cells were fixed by removing cell culture media and replacing it with 4% paraformaldehyde in PBS for 15–20 minutes at room temperature. After fixation, cells were washed three times with PBS and stored at 4°C until staining. To visualize nuclei, fixed cells were incubated in Hoechst 33342 for 15-20 minutes. Cells were imaged using a Nikon Eclipse Ti inverted microscope for chemotherapeutic treatment experiments and an Olympus confocal microscope with CellSens imaging software for higher magnification imaging. For experiments requiring immunostaining, additional staining steps including permeabilization, blocking, and primary and secondary antibody incubation were performed as detailed in the relevant results sections.

Cell and Nuclear Morphology

The images taken were analyzed using Fiji ImageJ (Schindelin et al., 2012) and CellProfiler (Stirling et al., 2021). Fiji ImageJ is an open-source software that can provide a description of the cell's geometry. This includes the area, perimeter, circularity, aspect ratio, roundness, and solidity. Fiji ImageJ measurements were taken after using the freehand selections tool to manually trace the outline of the cell body.

The nuclear morphology of cells was analyzed using CellProfiler, a free, open-source software designed by BROAD Institute. It allows users to quantitatively measure objects in hundreds of different 17 images in an automated manner, without manual tracing. This is done by building a

pipeline with tunable parameters, enabling users to optimize the settings for specific image sets. These parameters include different thresholding strategies and methods for distinguishing clumped objects. Once objects are identified based on the selected settings, in this case, the cell nuclei, geometric measurements are extracted and exported as a spreadsheet.

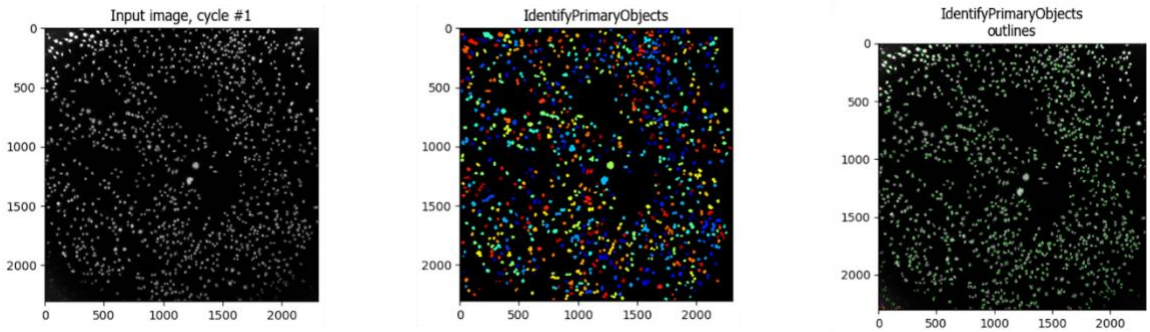

Figure 3. *Representative DAPI-stained images illustrating the CellProfiler image analysis pipeline. The original fluorescence image (left) serves as the input for automated nuclear detection (center), which generates segmented nuclear outlines (right) used to extract quantitative geometric measurements for each identified nucleus.*

Data Analysis and Statistics

All graphs and statistical analyses were performed using GraphPad Prism and RStudio. Nuclear morphology data, including mean nuclear area and form factor, were analyzed using Welch's unpaired t-test to compare hypoxic and normoxic conditions within each cell line, accounting for the unequal variances and large sample sizes characteristic of cell-level measurements. All statistical analyses were conducted at a 95% confidence interval. In figures, statistical significance is denoted by asterisks, where * corresponds to $p \leq 0.05$, ** corresponds to $p \leq 0.01$, *** corresponds to $p \leq 0.001$, and **** corresponds to $p \leq 0.0001$. Non-significance is denoted as "ns" where $p > 0.05$. For experiments with fewer than three biological replicates, statistical comparisons

were not performed and results are presented as descriptive statistics only. Error bars in all graphs represent the standard error of the mean (SEM).

Chapter 3: Results

Characterizing Nuclear Morphology Under Hypoxic and Normoxic Conditions

A hypoxia study was conducted to characterize the nuclear morphology of ID8 BRCA1, ID8 BRCA2, and ID8 C3 control cells under hypoxic (2% O_2) and normoxic conditions without treatment. Establishing baseline measurements of nuclear morphology under these two oxygen conditions sets the standard for understanding how hypoxia influences nuclear characteristics prior to any drug treatment.

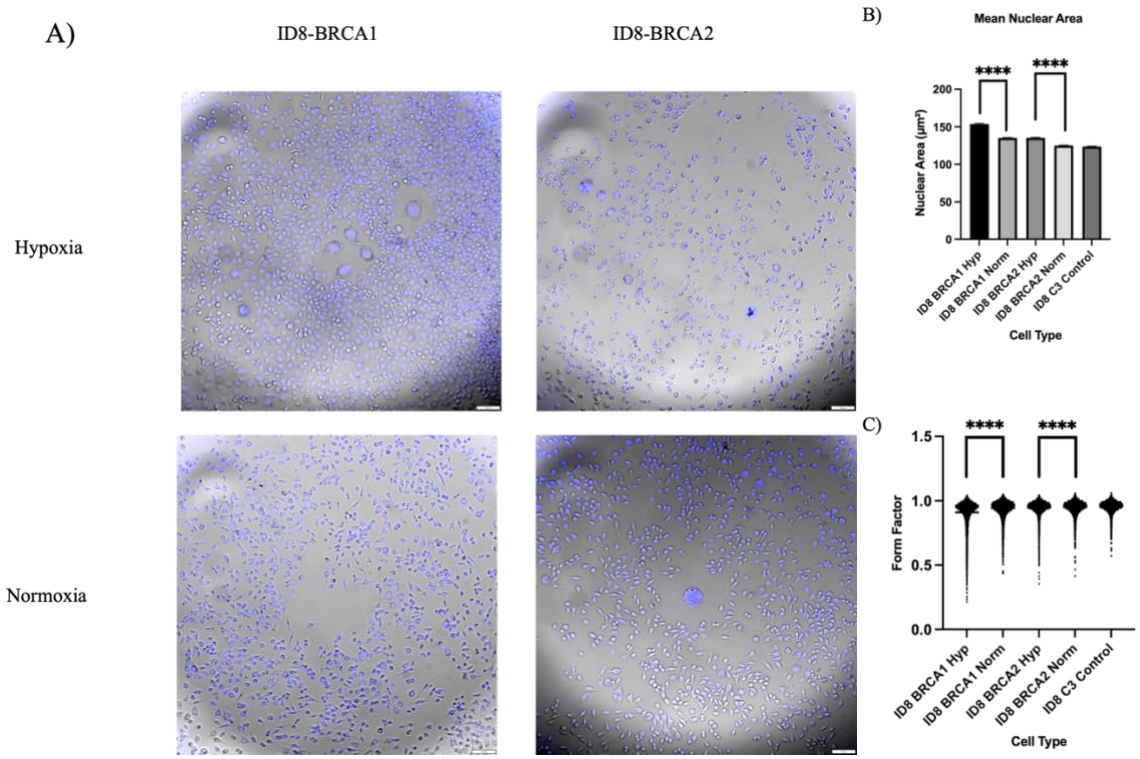

Figure 4. *Nuclear morphology of ID8 BRCA1, ID8 BRCA2, and ID8 C3 control cells under hypoxia and normoxia (N=1). A) Representative 10x magnification DAPI-stained images of ID8 BRCA1, ID8 BRCA2, and ID8 C3 control cells under hypoxic and normoxic conditions. Occasional enlarged nuclei consistent with PGCC morphology are visible across conditions. Scale*

*bar = 100 µm. B) Mean nuclear area for each condition. C) Form factor for each condition, where a value of 1 indicates a perfect circle. Statistical comparisons were performed using Welch's unpaired t-test. ****p < 0.001. n = 9,268-14,883 cells per condition.*

Thousands of nuclei from all three cell lines were analyzed across both oxygen conditions. Representative DAPI-stained images show largely uniform nuclear morphology across conditions, with occasional enlarged nuclei consistent with PGCC characteristics (Figure 4A). Quantitative analysis revealed that cells cultured under hypoxia demonstrated significantly larger mean nuclear areas compared to their normoxic counterparts, with this difference reaching statistical significance in both ID8 BRCA1 (153.8 µm² vs 135.4 µm², $p < 0.0001$) and ID8 BRCA2 cells (135.4 µm² vs 124.9 µm², $p < 0.0001$) (Figure 4B). The ID8 C3 control cells had the smallest mean nuclear area of 123.6 µm², consistent with a wildtype baseline. These findings suggest that hypoxia promotes nuclear enlargement in BRCA-mutant cells, with the effect being most pronounced in ID8 BRCA1 cells.

Form factor analysis revealed that hypoxic conditions were associated with more elongated nuclear morphology in both mutant cell lines (Figure 4C). ID8 BRCA1 cells showed the greatest reduction in form factor under hypoxia (0.9100 vs 0.9438, $p < 0.0001$), while ID8 BRCA2 cells showed a smaller but still statistically significant reduction (0.9471 vs 0.9510, $p < 0.0001$). The ID8 C3 control cells maintained the highest form factor of 0.9556, indicating the most circular nuclear morphology overall. Together, these results suggest that hypoxia preferentially drives nuclear irregularity in BRCA1-mutant cells.

PGCC Formation Under Hypoxic and Normoxic Conditions

To further characterize the effect of hypoxia on PGCC formation, the percentage of PGCCs was quantified across all three cell lines under normoxic and hypoxic conditions. Cells were considered PGCCs if their nuclear area was 2.5 times larger than the mean nuclear area of each respective parent cell line under the corresponding oxygen condition, as outlined in Table 1.

Table 1. PGCC thresholds for each condition

Parent Cells	PGCC Threshold (μm²)
ID8 BRCA1 Hyp	384.5
ID8 BRCA1 Norm	338.5
ID8 BRCA2 Hyp	338.5
ID8 BRCA2 Norm	312.25

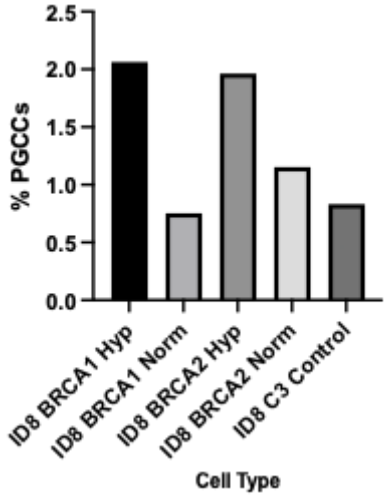

Figure 5. *Percentage of PGCCs in ID8 BRCA1, ID8 BRCA2, and ID8 C3 control cells under normoxia and hypoxia (N=1). A) Percentage of PGCCs per condition. Statistical comparisons could not be performed as only a single value per condition was obtained.*

Under normoxic conditions, ID8 BRCA1 cells showed a PGCC percentage of 0.75%, while ID8 BRCA2 cells showed 1.15% and ID8 C3 control cells showed 0.83%. Under hypoxic conditions, PGCC percentages were elevated in both BRCA-mutant cell lines compared to normoxia, with ID8 BRCA1 cells showing 2.06% and ID8 BRCA2 cells showing 1.96% (Figure 5). The ID8 C3 control cells maintained the lowest PGCC percentage overall at 0.83%, consistent with a wildtype baseline. These observations suggest that hypoxia may promote PGCC formation in BRCA-mutant cells, and that BRCA mutation status may influence baseline PGCC formation even under normoxic conditions.

PGCC Formation in ID8 BRCA1 and BRCA2 Cells Under Normoxia Following Paclitaxel and Carboplatin Treatment

To assess whether PGCC formation following chemotherapeutic treatment was specific to hypoxic conditions or occurred independently of oxygen levels, ID8 BRCA1 and ID8 BRCA2 cells were treated with 500nM PTX, 100µM Carboplatin (CPTN), and 50µM Carboplatin (CPTN) under normoxic conditions. Nuclear morphology was assessed across three biological replicates and compared against untreated normoxic baseline values established in Figure 4.

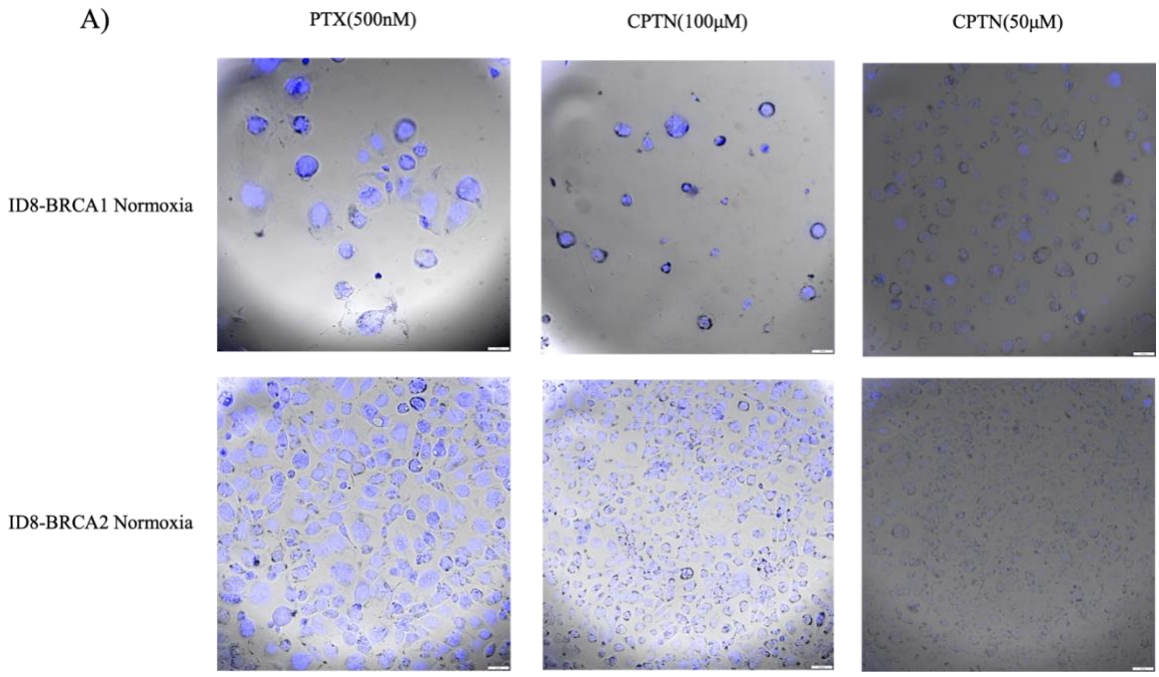

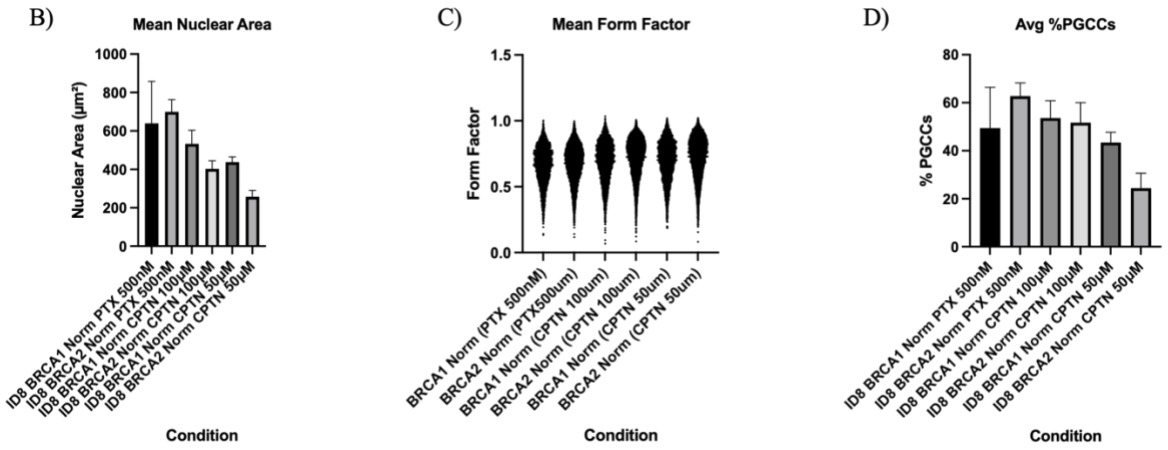

Figure 6. *Nuclear morphology of ID8 BRCA1 and ID8 BRCA2 cells under normoxia following 500nM PTX and Carboplatin treatment (N=3 for 500nM PTX and 100µM CPTN; N=2 for 50µM CPTN). A) Representative 10x magnification DAPI-stained images of ID8 BRCA1 and ID8 BRCA2 cells treated with 500nM PTX, 100µM CPTN, and 50µM CPTN under normoxic conditions. Enlarged nuclei consistent with PGCC morphology are visible across all treatment conditions. Scale bar = 100µm. B) Mean nuclear area for each condition. C) Form factor for each condition, where a value of 1 indicates a perfect circle. D) Percentage of PGCCs per condition. Cells were considered PGCCs if their nuclear area was 2.5 times larger than the mean nuclear area of the respective untreated parent cell line under normoxic conditions.*

Representative DAPI-stained images revealed widespread nuclear enlargement following treatment under normoxic conditions in both cell lines, consistent with PGCC formation across all treatment groups (Figure 6A). Mean nuclear area was elevated compared to untreated normoxic baseline values (BRCA1: 135.4 µm², BRCA2: 124.9 µm²) across all conditions. 500nM PTX produced the greatest nuclear enlargement in BRCA2 (699.2 µm²) followed by BRCA1 (639.9 µm²) cells. Among Carboplatin conditions, 100µM CPTN produced larger mean nuclear areas (BRCA1: 533.3 µm², BRCA2: 402.7 µm²) compared to 50µM CPTN (BRCA1: 437.8 µm²,

BRCA2: 257.6 μm²), consistent with a dose-dependent effect (Figure 6B). Notably, BRCA2 cells treated with 50μM CPTN showed the smallest mean nuclear area across all normoxic treatment conditions (257.6 μm²), suggesting a differential response between cell lines at lower Carboplatin concentrations.

Form factor analysis revealed a marked reduction in nuclear circularity across all treatment conditions compared to untreated normoxic cells (BRCA1 baseline: 0.9438, BRCA2 baseline: 0.9510), indicating that treated nuclei were substantially more irregular in shape regardless of oxygen conditions (Figure 6C). 500nM PTX produced the lowest form factor values in both BRCA1 (0.662) and BRCA2 (0.673) cells, while Carboplatin-treated cells showed slightly higher form factors ranging from 0.690 to 0.729, consistent with the pattern observed under hypoxia.

The percentage of PGCCs was markedly elevated across all normoxic treatment conditions compared to untreated normoxic baseline values of approximately 0.75% for BRCA1 and 1.15% for BRCA2 (Figure 6D). Under 500nM PTX treatment, BRCA1 cells showed a mean PGCC percentage of 48.11% and BRCA2 cells showed 62.69%. 100μM CPTN produced mean PGCC percentages of 53.66% in BRCA1 and 51.70% in BRCA2 cells, while 50μM CPTN yielded 43.46% in BRCA1 and 24.47% in BRCA2 cells. Notably, comparison with hypoxic treatment conditions (Figure 7) revealed that PGCC formation was similarly elevated under both oxygen conditions, suggesting that chemotherapy-induced PGCC formation occurs independently of hypoxia in these BRCA-mutant cell lines. This is a particularly important finding as it suggests that the chemotherapeutic drugs themselves, rather than the hypoxic microenvironment, are the primary drivers of PGCC induction.

PGCC Formation in ID8 BRCA1 and BRCA2 Cells Under Hypoxia Following Paclitaxel and Carboplatin Treatment

To investigate the effect of chemotherapeutic treatment on PGCC formation under hypoxic conditions, ID8 BRCA1 and ID8 BRCA2 cells were treated with 500nM PTX, 100µM Carboplatin (CPTN), and 50µM Carboplatin (CPTN) under hypoxia (2% O_2). Nuclear morphology was assessed across two biological replicates and compared against untreated hypoxic baseline values established in Figure 4.

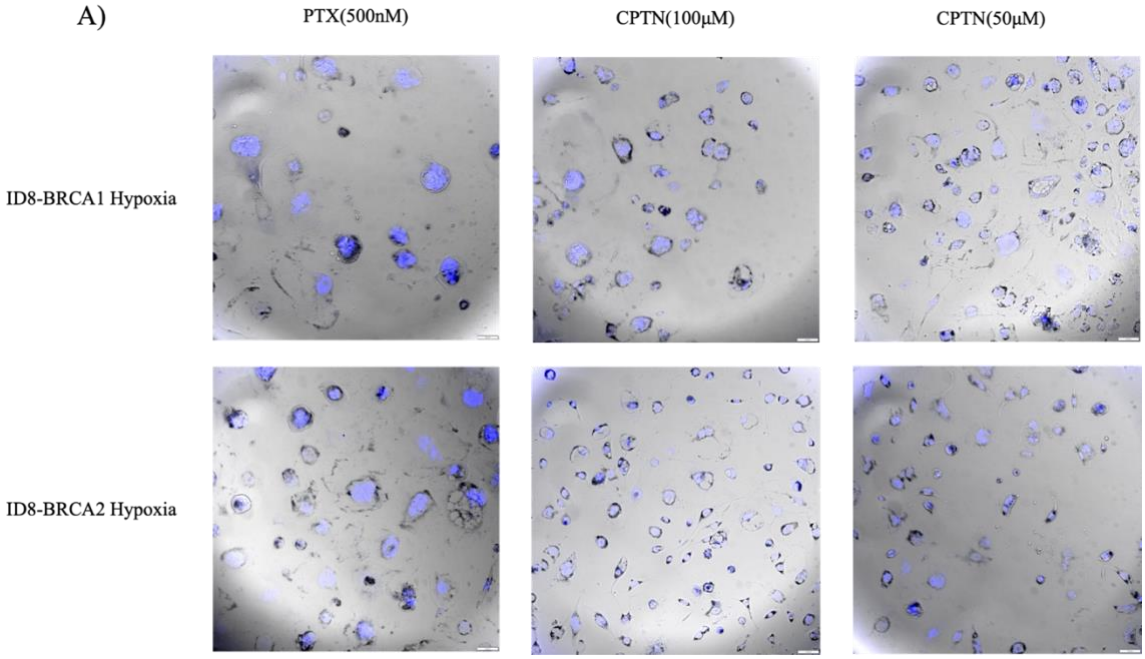

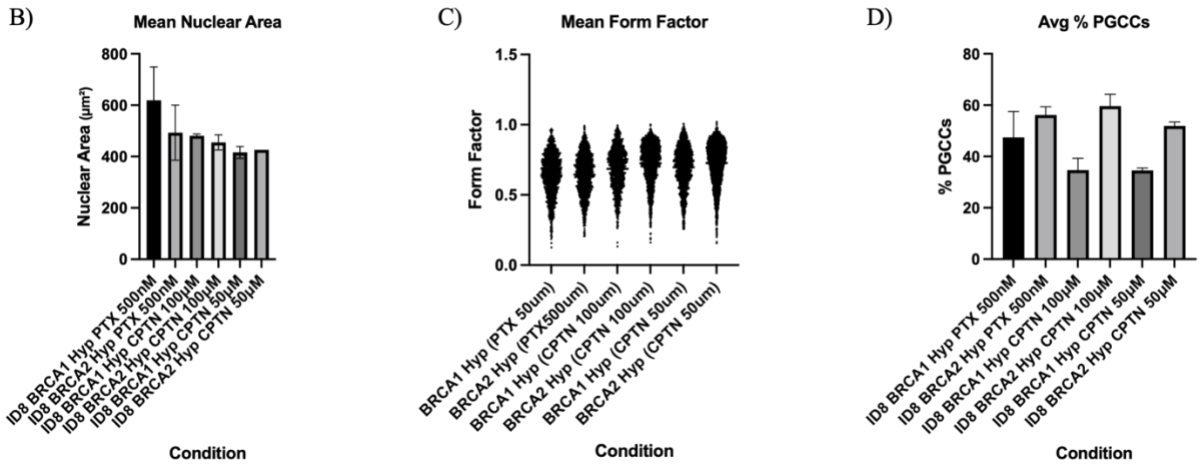

Figure 7. *Nuclear morphology of ID8 BRCA1 and ID8 BRCA2 cells under hypoxia following 500nM PTX and Carboplatin treatment (N=2 for 500nM PTX, 100µM CPTN and 50µM CPTN BRCA1; N=1 for 50µM CPTN BRCA2). A) Representative 10x magnification DAPI-stained images of ID8 BRCA1 and ID8 BRCA2 cells treated with 500nM PTX, 100µM CPTN, and 50µM CPTN under hypoxic conditions. Enlarged nuclei consistent with PGCC morphology are visible across all treatment conditions. Scale bar = 100µm. B) Mean nuclear area for each condition. C) Form factor for each condition, where a value of 1 indicates a perfect circle. D) Percentage of PGCCs per condition. Cells were considered PGCCs if their nuclear area was 2.5 times larger than the mean nuclear area of the respective untreated parent cell line under hypoxic conditions.*

Representative DAPI-stained images revealed a striking increase in the number and size of enlarged nuclei following treatment under hypoxia in both cell lines, consistent with widespread PGCC formation across all treatment conditions (Figure 7A). Mean nuclear area was elevated compared to untreated hypoxic baseline values (BRCA1: 153.8 µm², BRCA2: 135.4 µm²) across all conditions. 500nM PTX produced the greatest nuclear enlargement in BRCA1 (619.3 µm²) cells, while BRCA2 cells showed comparable enlargement under 500nM PTX (492.9 µm²). Among Carboplatin conditions, 100µM CPTN produced larger mean nuclear areas (BRCA1:

480.8 μm², BRCA2: 454.5 μm²) compared to 50μM CPTN (BRCA1: 415.5 μm², BRCA2: 425.7 μm²), consistent with a dose-dependent relationship for Carboplatin (Figure 7B).

Form factor analysis revealed a pronounced reduction in nuclear circularity across all treatment conditions compared to untreated hypoxic cells (BRCA1 baseline: 0.9100, BRCA2 baseline: 0.9471), indicating that treated nuclei were not only larger but also considerably more irregular in shape (Figure 7C). 500nM PTX produced the lowest form factor values in both BRCA1 (0.640) and BRCA2 (0.643) cells, while Carboplatin-treated cells showed slightly higher but still markedly reduced form factors ranging from 0.682 to 0.722, consistent with the aberrant nuclear morphology characteristic of PGCCs.

The percentage of PGCCs increased following all treatments compared to untreated hypoxic baseline values of approximately 2.06% for BRCA1 and 1.96% for BRCA2 (Figure 7D). Under 500nM PTX treatment, BRCA1 cells showed a mean PGCC percentage of 47.42% and BRCA2 cells showed 56.19%. 100μM CPTN produced mean PGCC percentages of 34.69% in BRCA1 and 59.66% in BRCA2 cells, while 50μM CPTN yielded 34.56% in BRCA1 and 53.46% in BRCA2 cells. Across all treatment conditions, BRCA2 cells consistently showed a higher propensity for PGCC formation compared to BRCA1 cells. Notably, comparison with normoxic treatment conditions (Figure 6) revealed that PGCC formation was similarly elevated under both oxygen conditions, suggesting that chemotherapy-induced PGCC formation occurs independently of hypoxia in these BRCA-mutant cell lines.

H2AX Expression in Hypoxia-Treated ID8 BRCA1 and BRCA2 Cells Following Chemotherapy

To characterize total H2A.X protein distribution in PGCC-enriched populations following chemotherapeutic treatment under hypoxic conditions, ID8 BRCA1 and ID8 BRCA2 cells were stained with an anti-H2A.X antibody targeting total H2A.X protein (Histone H2A.X D17A3 XP® Rabbit mAb, Cell Signaling Technology, 1:500), Phalloidin-AF647 (1:400), and Hoechst (1:500) following treatment with 500nM PTX, 100µM Carboplatin (CPTN), and 50µM Carboplatin (CPTN) under hypoxia (2% O_2). It should be noted that this antibody detects total H2A.X protein and is not specific to the phosphorylated form (γH2AX), and therefore the results presented here reflect total H2A.X chromatin incorporation rather than a direct measure of DNA damage signaling.

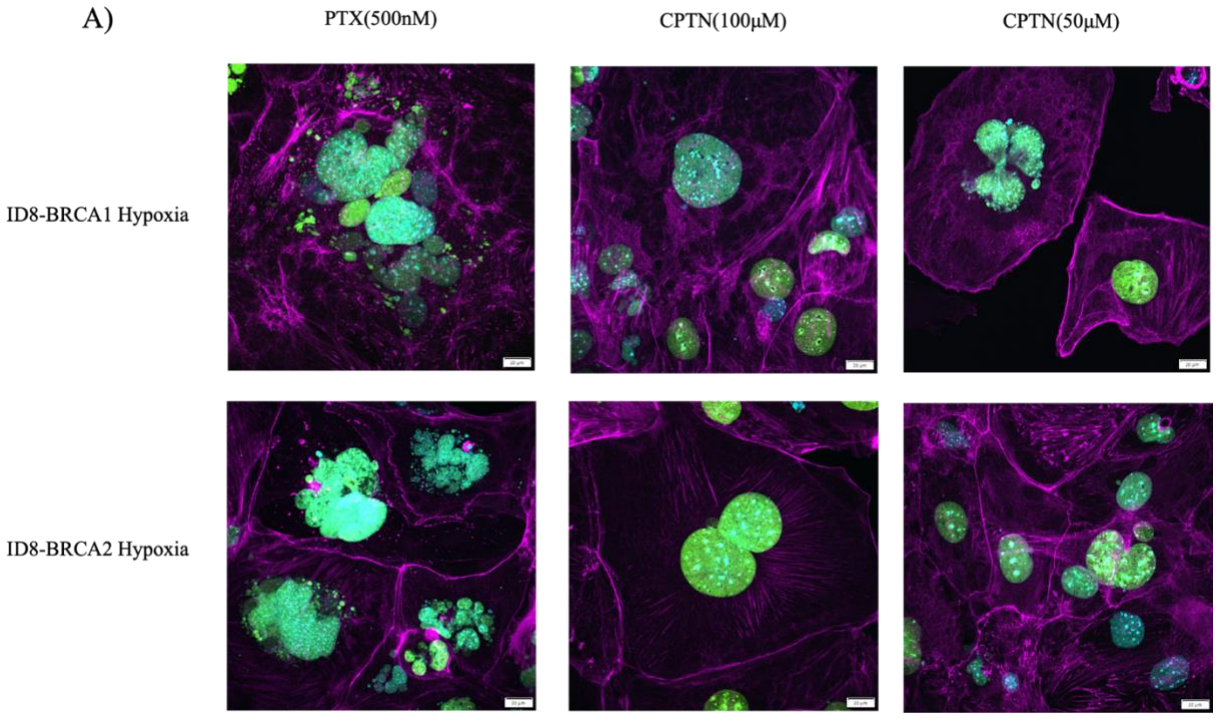

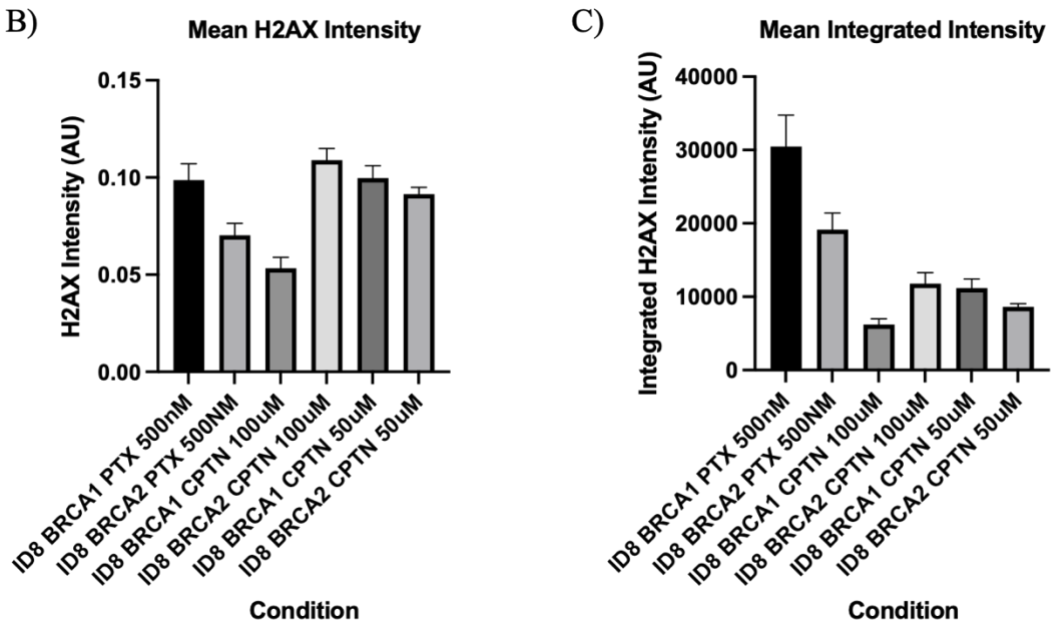

Figure 8. *H2AX expression in hypoxia-treated ID8 BRCA1 and ID8 BRCA2 cells following chemotherapy (N=1). A) Representative 60x magnification immunofluorescence images of ID8 BRCA1 and ID8 BRCA2 cells treated with 500nM PTX, 100μM CPTN, and 50μM CPTN under hypoxic conditions. Cyan = Hoechst (nuclei), Green = H2AX (DNA damage marker), Magenta = Phalloidin (F-actin). Scale bar = 20μm. B) Mean H2AX intensity per condition. C) Integrated H2AX intensity per condition, representing the total H2AX signal across the entire nucleus.*

Representative immunofluorescence images revealed large, morphologically distinct PGCC nuclei across all treatment conditions in both cell lines, with diffuse H2A.X signal visible across the enlarged nuclei consistent with broad chromatin-associated H2A.X distribution (Figure 8A). The H2A.X signal was particularly prominent in 500nM PTX-treated cells, where nuclei appeared most enlarged and irregular in both BRCA1 and BRCA2 cell lines.

Mean total H2A.X intensity varied across treatment conditions and cell lines (Figure 8B). BRCA1 cells treated with 50μM CPTN showed the highest mean H2A.X intensity (0.0997), followed

closely by 500nM PTX-treated BRCA1 cells (0.0987). BRCA2 cells treated with 100μM CPTN showed the highest mean H2A.X intensity among BRCA2 conditions (0.1089), while 500nM PTX-treated BRCA2 cells showed a lower mean intensity (0.0703). Overall, H2A.X intensity values ranged from 0.0533 to 0.1089 AU across all conditions, with no single treatment consistently producing the highest H2A.X signal across both cell lines.

Integrated total H2A.X intensity, which reflects the total H2A.X signal across the entire nucleus and accounts for the enlarged chromatin content characteristic of PGCCs, revealed notably higher values in 500nM PTX-treated cells compared to Carboplatin-treated conditions (Figure 8C). BRCA1 cells treated with 500nM PTX showed the highest integrated H2A.X intensity (30,471 AU), followed by BRCA2 cells treated with 500nM PTX (19,139 AU). Among Carboplatin conditions, 100μM CPTN produced higher integrated intensities in BRCA2 cells (11,771 AU) compared to BRCA1 cells (6,204 AU), while 50μM CPTN showed comparable values between BRCA1 (11,191 AU) and BRCA2 (8,603 AU) cells. The elevated integrated H2A.X intensities observed under 500nM PTX treatment are consistent with the larger nuclear and chromatin content in these cells, reflecting a greater total H2A.X signal across the expanded PGCC chromatin. These findings demonstrate that total H2A.X protein is broadly distributed across the chromatin of chemotherapy-treated PGCCs under hypoxic conditions. As this represents a single experiment, these findings should be interpreted with caution and replicated to draw definitive conclusions.

Chapter 4: Discussion and Future Directions

It has been established that BRCA1 and BRCA2 mutations are among the most clinically significant genetic alterations in epithelial ovarian cancer, contributing to impaired homologous recombination repair and heightened genomic instability. Based on the experiments conducted in this study, the results are consistent with those observations, as BRCA-mutant cells exhibited pronounced nuclear morphological changes and substantial PGCC formation across multiple experimental conditions.

Hypoxia is a well-documented feature of the ovarian tumor microenvironment and has been shown to promote replication stress and impair DNA damage repair pathways. The significant increases in nuclear area and reductions in form factor observed under hypoxic conditions in both BRCA1 and BRCA2 cells compared to their normoxic counterparts are consistent with this, suggesting that oxygen deprivation exacerbates the nuclear instability already present in BRCA-mutant cells. The BRCA1 cell line appeared more sensitive to hypoxia-induced nuclear changes than BRCA2 cells, which is biologically plausible given the distinct roles of these two proteins in the DNA damage response. BRCA1 functions more broadly in cell cycle checkpoint regulation and DNA end resection, and its loss may leave cells less equipped to manage the replication stress imposed by hypoxia. Additionally, comparison with the C3 wildtype control cells in the first set of experiments confirmed that these nuclear changes are specific to the BRCA-mutant context, as C3 cells maintained smaller nuclear areas and higher form factors across both oxygen conditions, consistent with a more stable nuclear phenotype in the absence of BRCA mutations.

The elevation of PGCC percentage under hypoxia in both BRCA-mutant cell lines supports the idea that BRCA mutation status may promote PGCC formation even in the absence of treatment. PGCCs are known to arise through mechanisms including endoreduplication and mitotic slippage,

both of which are favored under conditions of genomic stress. Without functional homologous recombination repair, BRCA-mutant cells may be more prone to the aberrant cell divisions that give rise to these giant cells. Future studies should directly confirm polyploidy in the identified PGCC population through DNA content analysis such as flow cytometry with propidium iodide staining, as nuclear area alone - while an established and practical metric - does not directly confirm increased genomic content or provide quantitative measurements of ploidy.

Perhaps the most striking finding of this study was the substantial induction of PGCCs following chemotherapeutic treatment with Paclitaxel and Carboplatin under both normoxic and hypoxic conditions. PGCC percentages reached as high as 63% under normoxia and 60% under hypoxia across both cell lines and treatment conditions, representing a dramatic increase from untreated baseline values of approximately 0.75-2.06%. This degree of PGCC induction by standard-of-care chemotherapeutic agents is particularly concerning from a clinical standpoint, as PGCCs have been shown to exhibit chemoresistant properties and the ability to promote tumor regrowth following treatment (Mirzayans & Murray, 2023). The observation that PGCC formation was similarly elevated under both hypoxic and normoxic conditions suggests that chemotherapy-induced PGCC formation in these BRCA-mutant cell lines occurs largely independently of the hypoxic microenvironment. This implies that the BRCA mutation itself, rather than oxygen deprivation, may be the primary driver of this response - a hypothesis that warrants direct testing in future experiments. Comparing PGCC formation rates between BRCA1 and BRCA2 cells across treatment conditions could also help clarify whether one mutation confers a greater propensity for chemotherapy-induced PGCC formation than the other, which could have implications for understanding differential treatment responses in patients with specific BRCA mutations.

The nuclear area and form factor data from treated cells further supported the shift toward a PGCC phenotype following chemotherapy. 500nM PTX, a microtubule-stabilizing agent that disrupts normal mitotic spindle assembly, produced the largest nuclear areas in both cell lines under both oxygen conditions, while Carboplatin, a platinum-based DNA crosslinking agent, produced a dose-dependent effect on nuclear area. Although the two drugs act through distinct mechanisms, both appear to strongly promote PGCC formation in BRCA-mutant ovarian cancer cells, which is consistent with broader observations in the field that chemotherapy can paradoxically enrich for resistant PGCC populations. The consistently lower form factor values in treated cells relative to untreated baseline values indicate that treatment-induced nuclei are not only larger but also substantially more irregular in shape, further supporting a transition toward a PGCC-like morphology. It would be interesting to explore whether these morphological differences between drug types reflect distinct biological mechanisms of PGCC formation - for example, whether 500nM PTX promotes PGCC formation predominantly through mitotic slippage while Carboplatin acts more through endoreduplication - as this could inform the design of combination therapies aimed at preventing PGCC enrichment during treatment.

The total H2A.X immunofluorescence staining revealed broad chromatin-associated H2A.X distribution within PGCC nuclei across all treatment conditions in both BRCA1 and BRCA2 cells under hypoxic conditions. As the antibody used in this study detects total H2A.X protein rather than the phosphorylated γH2AX form, the results reflect H2A.X chromatin incorporation across the enlarged PGCC nuclei rather than direct DNA damage signaling. The elevated integrated H2A.X intensities observed under 500nM PTX treatment are consistent with the larger chromatin content in PTX-treated PGCCs, as larger nuclei with greater DNA content would be expected to incorporate more total H2A.X protein. Future experiments should employ a phospho-specific anti-

γH2AX antibody targeting Ser139 phosphorylation to directly assess DNA damage signaling within these PGCC populations, which would provide a more definitive measure of the genomic damage sustained by these cells following chemotherapeutic treatment under hypoxic conditions.

Several important limitations must be acknowledged. The only metric used to identify PGCCs in this study was nuclear area, which - while a practical and established approach - does not directly confirm polyploidy. Future work should incorporate DNA content analysis to confirm that the identified PGCC population is truly polyploid. It would also be valuable to assess the functional properties of these treatment-induced PGCCs through cell viability assays or isolation and re-treatment experiments to directly test whether they exhibit enhanced chemoresistance relative to the broader cell population. Given that PGCCs contribute to heterogeneity in the tumor microenvironment and have exhibited the ability to promote tumor regrowth after treatment (Mirzayans & Murray, 2023), understanding the conditions that favor their formation in the context of BRCA mutations and standard chemotherapy is an important step toward developing strategies to prevent or exploit this phenomenon therapeutically.

Chapter 5: Conclusion

The experiments conducted in this thesis were designed to investigate how hypoxia and BRCA mutation status influence nuclear morphology and PGCC formation in epithelial ovarian cancer cells, and to explore how standard chemotherapeutic agents interact with these parameters. Through quantitative image analysis, nuclear morphometric analysis, and immunofluorescence staining, this work provides preliminary evidence that hypoxia promotes nuclear enlargement and irregularity in BRCA-mutant cells, that BRCA mutation status may predispose cells to elevated baseline PGCC formation, and that treatment with 500nM PTX and Carboplatin substantially amplifies PGCC induction in both cell lines regardless of oxygen conditions. The trends observed across experiments are consistent and point toward biologically meaningful phenomena that merit further investigation. Moving forward, increasing biological replicates, incorporating additional approaches for DNA content analysis and DNA damage analysis, and extending the immunostaining experiments to normoxic treated conditions will be critical steps in strengthening the conclusions that can be drawn from this work.

Ovarian cancer carries a disproportionately high mortality rate relative to its incidence, in large part because it is frequently diagnosed at an advanced stage and because resistance to standard chemotherapy remains a persistent clinical challenge. The presence of BRCA1 and BRCA2 mutations adds an additional layer of complexity, as these mutations alter the fundamental biology of how cells respond to DNA damage and genomic stress. Understanding how BRCA-mutant ovarian cancer cells respond to tumor microenvironment-relevant conditions, including hypoxia, and to commonly used chemotherapeutic agents is critical in improving patient outcomes. The results of this thesis suggest that chemotherapy may inadvertently enrich for PGCCs that have the capacity to survive significant genomic damage and potentially re-emerge as a more resistant

population of cancer cells, which has direct implications for how treatment strategies are designed and evaluated.

Cancer research is increasingly moving toward precision medicine, where treatment decisions are guided by the specific molecular and phenotypic characteristics of an individual patient's tumor. The findings of this thesis contribute to this effort by highlighting PGCC formation as a phenotypic response to chemotherapy that may be particularly pronounced in the setting of BRCA mutations. If the mechanisms underlying chemotherapy-induced PGCC formation can be fully elucidated, strategies that either prevent PGCC induction during treatment or selectively eliminate the surviving PGCC population could offer a meaningful improvement in therapeutic efficacy for patients with BRCA-mutant ovarian cancer. Characterizing these outlier populations and the conditions that give rise to them is a necessary step toward developing treatments that account for the full complexity of tumor heterogeneity rather than targeting only the dominant cell population.

References:

1. National Cancer Institute. What is cancer? National Cancer Institute. Published October 11, 2021. https://www.cancer.gov/about-cancer/understanding/what-is-cancer

2. Hanahan D, Weinberg RA. The hallmarks of cancer. Cell. 2000 Jan 7;100(1):57-70. doi: 10.1016/s0092-8674(00)81683-9. PMID: 10647931.

3. Hanahan D, Weinberg RA. Hallmarks of cancer: the next generation. Cell. 2011 Mar 4;144(5):646-74. doi: 10.1016/j.cell.2011.02.013. PMID: 21376230.

4. World Health Organization. Cancer. WHO. Published February 3, 2022. https://www.who.int/news-room/fact-sheets/detail/cancer

Bray F, Laversanne M, Sung H, Ferlay J, Siegel RL, Soerjomataram I, Jemal A. Global cancer statistics 2022: GLOBOCAN estimates of incidence and mortality worldwide for 36 cancers in 185 countries. CA Cancer J Clin. 2024 May-Jun;74(3):229-263. doi: 10.3322/caac.21834. Epub 2024 Apr 4. PMID: 38572751.

6. American Cancer Society. Key statistics for ovarian cancer. Published January 19, 2024. https://www.cancer.org/cancer/types/ovarian-cancer/about/key-statistics.html

7. National Cancer Institute. Cancer stat facts: Ovarian cancer. SEER Program. https://seer.cancer.gov/statfacts/html/ovary.html

8. Wallis B, Bowman KR, Lu P, Lim CS. The Challenges and Prospects of p53-Based Therapies in Ovarian Cancer. Biomolecules. 2023 Jan 12;13(1):159. doi: 10.3390/biom13010159. PMID: 36671544; PMCID: PMC9855757.

9. Kim J, Park EY, Kim O, Schilder JM, Coffey DM, Cho CH, Bast RC Jr. Cell Origins of High-Grade Serous Ovarian Cancer. Cancers (Basel). 2018 Nov 12;10(11):433. doi: 10.3390/cancers10110433. PMID: 30424539; PMCID: PMC6267333.

10. Matulonis UA, Sood AK, Fallowfield L, Howitt BE, Sehouli J, Karlan BY. Ovarian cancer. Nat Rev Dis Primers. 2016 Aug 25;2:16061. doi: 10.1038/nrdp.2016.61. PMID: 27558151; PMCID: PMC7290868.

11. Ahmed AA, Etemadmoghadam D, Temple J, Lynch AG, Riad M, Sharma R, Stewart C, Fereday S, Caldas C, Defazio A, Bowtell D, Brenton JD. Driver mutations in TP53 are ubiquitous in high grade serous carcinoma of the ovary. J Pathol. 2010 May;221(1):49-56. doi: 10.1002/path.2696. PMID: 20229506; PMCID: PMC3262968.

12. Launonen IM, Lyytikäinen N, Casado J, Anttila EA, Szabó A, Haltia UM, Jacobson CA, Lin JR, Maliga Z, Howitt BE, Strickland KC, Santagata S, Elias K, D'Andrea AD, Konstantinopoulos PA, Sorger PK, Färkkilä A. Single-cell tumor-immune microenvironment of BRCA1/2 mutated high-grade serous ovarian cancer. Nat Commun. 2022 Feb 11;13(1):835. doi: 10.1038/s41467-022-28389-3. PMID: 35149709; PMCID: PMC8837628.

13. Kotnik EN, Mullen MM, Spies NC, Li T, Inkman M, Zhang J, Martins-Rodrigues F, Hagemann IS, McCourt CK, Thaker PH, Hagemann AR, Powell MA, Mutch DG, Khabele D, Longmore GD, Mardis ER, Maher CA, Miller CA, Fuh KC. Genetic characterization of primary and metastatic high-grade serous ovarian cancer tumors reveals distinct features associated with survival. Commun Biol. 2023 Jul 3;6(1):688. doi: 10.1038/s42003-023-05026-3. PMID: 37400526; PMCID: PMC10318066.

14. Arcieri M, Tius V, Andreetta C, Restaino S, Biasioli A, Poletto E, Damante G, Ercoli A, Driul L, Fagotti A, Lorusso D, Scambia G, Vizzielli G. How BRCA and homologous recombination deficiency change therapeutic strategies in ovarian cancer: a review of literature. Front Oncol. 2024 Mar 8;14:1335196. doi: 10.3389/fonc.2024.1335196. PMID: 38525421; PMCID: PMC10957789.

15. Ledermann JA. First-line treatment of ovarian cancer: questions and controversies to address. Ther Adv Med Oncol. 2018 Apr 11;10:1758835918768232. doi: 10.1177/1758835918768232. PMID: 29662548; PMCID: PMC5898654.

16. Ozols RF, Bundy BN, Greer BE, Fowler JM, Clarke-Pearson D, Burger RA, Mannel RS, DeGeest K, Hartenbach EM, Baergen R; Gynecologic Oncology Group. Phase III trial of carboplatin and paclitaxel compared with cisplatin and paclitaxel in patients with optimally resected stage III ovarian cancer: a Gynecologic Oncology Group study. J Clin Oncol. 2003 Sep 1;21(17):3194-200. doi: 10.1200/JCO.2003.02.153. Epub 2003 Jul 14. PMID: 12860964.

17. Tchounwou PB, Dasari S, Noubissi FK, Ray P, Kumar S. Advances in Our Understanding of the Molecular Mechanisms of Action of Cisplatin in Cancer Therapy. J Exp Pharmacol. 2021 Mar 18;13:303-328. doi: 10.2147/JEP.S267383. PMID: 33776489; PMCID: PMC7987268.

18. Basu A, Krishnamurthy S. Cellular responses to Cisplatin-induced DNA damage. J Nucleic Acids. 2010 Aug 8;2010:201367. doi: 10.4061/2010/201367. PMID: 20811617; PMCID: PMC2929606.

19. Awosika AO, Farrar MC, Jacobs TF. Paclitaxel. 2023 Nov 18. In: StatPearls [Internet]. Treasure Island (FL): StatPearls Publishing; 2026 Jan–. PMID: 30725602.

20. Barretina-Ginesta MP. DNA damaging agents in ovarian cancer. EJC Suppl. 2020 Aug 22;15:67-72. doi: 10.1016/j.ejcsup.2020.06.001. PMID: 33240444; PMCID: PMC7573464.

21. Ovejero-Sánchez M, González-Sarmiento R, Herrero AB. DNA Damage Response Alterations in Ovarian Cancer: From Molecular Mechanisms to Therapeutic Opportunities. Cancers (Basel). 2023 Jan 10;15(2):448. doi: 10.3390/cancers15020448. PMID: 36672401; PMCID: PMC9856346.

22. Ponton-Almodovar A, Sanderson S, Rattan R, Bernard JJ, Horibata S. Ovarian tumor microenvironment contributes to tumor progression and chemoresistance. Cancer Drug Resist. 2024 Dec 17;7:53. doi: 10.20517/cdr.2024.111. PMID: 39802952; PMCID: PMC11724355.

23. Qi, R., Yang, J., Shen, S. *et al.* Role of the tumor microenvironment in chemotherapy resistance in ovarian cancer and targeted therapy. *J Ovarian Res* 19, 14 (2026). https://doi.org/10.1186/s13048-025-01927-5

24. Yang Y, Yang Y, Yang J, Zhao X and Wei X (2020) Tumor Microenvironment in Ovarian Cancer: Function and Therapeutic Strategy. Front. Cell Dev. Biol. 8:758. doi: 10.3389/fcell.2020.00758

25. Chen G, Wu K, Li H, Xia D and He T (2022) Role of hypoxia in the tumor microenvironment and targeted therapy. Front. Oncol. 12:961637. doi: 10.3389/fonc.2022.961637

26. Liu P, Wang L and Yu H (2024) Polyploid giant cancer cells: origin, possible pathways of formation, characteristics, and mechanisms of regulation. Front. Cell Dev. Biol. 12:1410637. doi: 10.3389/fcell.2024.1410637

27. Klemba A, Bodnar L, Was H, Brodaczewska KK, Wcislo G, Szczylik CA, Kieda C. Hypoxia-Mediated Decrease of Ovarian Cancer Cells Reaction to Treatment: Significance for Chemo- and Immunotherapies. Int J Mol Sci. 2020 Dec 14;21(24):9492. doi: 10.3390/ijms21249492. PMID: 33327450; PMCID: PMC7764929.

28. Zhang S, Mercado-Uribe I, Xing Z, Sun B, Kuang J, Liu J. Generation of cancer stem-like cells through the formation of polyploid giant cancer cells. Oncogene. 2014 Jan 2;33(1):116-28. doi: 10.1038/onc.2013.96. Epub 2013 Mar 25. Erratum in: Oncogene. 2014 Jan 2;33(1):134. PMID: 23524583; PMCID: PMC3844126.

29. Zhou X, Zhou M, Zheng M, Tian S, Yang X, Ning Y, Li Y and Zhang S (2022) Polyploid giant cancer cells and cancer progression. Front. Cell Dev. Biol. 10:1017588. doi: 10.3389/fcell.2022.1017588

30. Shu Z, Row S, Deng WM. Endoreplication: The Good, the Bad, and the Ugly. Trends Cell Biol. 2018 Jun;28(6):465-474. doi: 10.1016/j.tcb.2018.02.006. Epub 2018 Mar 19. PMID: 29567370; PMCID: PMC5962415.

31. Song Y, Zhao Y, Deng Z, Zhao R, Huang Q. Stress-Induced Polyploid Giant Cancer Cells: Unique Way of Formation and Non-Negligible Characteristics. Front Oncol. 2021 Aug 30;11:724781. doi: 10.3389/fonc.2021.724781. PMID: 34527590; PMCID: PMC8435787.

32. Liu J, Erenpreisa J, Sikora E. Polyploid giant cancer cells: An emerging new field of cancer biology. Semin Cancer Biol. 2022 Jun;81:1-4. doi: 10.1016/j.semcancer.2021.10.006. Epub 2021 Oct 22. PMID: 34695579.

33. Casotti MC, Meira DD, Zetum ASS, Araújo BC, Silva DRCD, Santos EVWD, Garcia FM, Paula F, Santana GM, Louro LS, Alves LNR, Braga RFR, Trabach RSDR, Bernardes SS, Louro TES, Chiela ECF, Lenz G, Carvalho EF, Louro ID. Computational Biology Helps Understand How Polyploid Giant Cancer Cells Drive Tumor Success. Genes (Basel). 2023 Mar 26;14(4):801. doi: 10.3390/genes14040801. PMID: 37107559; PMCID: PMC10137723.

34. Zhang X, Yao J, Li X, Niu N, Liu Y, Hajek RA, Peng G, Westin S, Sood AK, Liu J. Targeting polyploid giant cancer cells potentiates a therapeutic response and overcomes resistance to PARP inhibitors in ovarian cancer. Sci Adv. 2023 Jul 21;9(29):eadf7195. doi: 10.1126/sciadv.adf7195. Epub 2023 Jul 21. PMID: 37478190; PMCID: PMC10361597.

35. Mirzayans, Razmik, and David Murray. 2023. "Intratumor Heterogeneity and Treatment Resistance of Solid Tumors with a Focus on Polyploid/Senescent Giant Cancer Cells (PGCCs)" *International Journal of Molecular Sciences* 24, no. 14: 11534. https://doi.org/10.3390/ijms241411534

36. Walton J, Blagih J, Ennis D, Leung E, Dowson S, Farquharson M, Tookman LA, Orange C, Athineos D, Mason S, Stevenson D, Blyth K, Strathdee D, Balkwill FR, Vousden K, Lockley M, McNeish IA. CRISPR/Cas9-Mediated Trp53 and Brca2 Knockout to Generate Improved Murine Models of Ovarian High-Grade Serous Carcinoma. Cancer Res. 2016 Oct 15;76(20):6118-6129. doi: 10.1158/0008-5472.CAN-16-1272. Epub 2016 Aug 16. PMID: 27530326; PMCID: PMC5802386.

37. Manickasamy, M.K., Aswani, B.S., Banerjee, R. et al. Etiology of polyploid giant cancer cells: a new frontier in cancer biology. Cancer Cell Int 26, 84 (2026). https://doi.org/10.1186/s12935-025-04079-0

38. Bigos KJA, Quiles CG, Lunj S, Smith DJ, Krause M, Troost EGC, West CM, Hoskin P and Choudhury A (2024) Tumour response to hypoxia: understanding the hypoxic tumour microenvironment to improve treatment outcome in solid tumours. Front. Oncol. 14:1331355. doi: 10.3389/fonc.2024.1331355

39. Hosking, H., Pederick, W., Neilsen, P. and Fenning, A. (2024), Considerations for the Use of the DNA Damage Marker γ-H2AX in Disease Modeling, Detection, Diagnosis, and Prognosis. Aging and Cancer., 5: 62-69. https://doi.org/10.1002/aac2.12074

40. Valente D, Gentileschi MP, Guerrisi A, Bruzzaniti V, Morrone A, Soddu S, Verdina A. Factors to Consider for the Correct Use of γH2AX in the Evaluation of DNA Double-Strand Breaks Damage Caused by Ionizing Radiation. Cancers (Basel). 2022 Dec 15;14(24):6204. doi: 10.3390/cancers14246204. PMID: 36551689; PMCID: PMC9776434.

41. Xu Z, Xie H, Song L, Huang Y, Huang J. BRCA1 and BRCA2 in DNA damage and replication stress response: Insights into their functions, mechanisms, and implications for cancer treatment. DNA Repair (Amst). 2025 Jun;150:103847. doi: 10.1016/j.dnarep.2025.103847. Epub 2025 May 13. PMID: 40373656.

42. Jasin M, Rothstein R. Repair of strand breaks by homologous recombination. Cold Spring Harb Perspect Biol. 2013 Nov 1;5(11):a012740. doi: 10.1101/cshperspect.a012740. PMID: 24097900; PMCID: PMC3809576.

43. Caracciolo D, Riillo C, Di Martino MT, Tagliaferri P, Tassone P. Alternative Non-Homologous End-Joining: Error-Prone DNA Repair as Cancer's Achilles' Heel. Cancers. 2021; 13(6):1392. https://doi.org/10.3390/cancers13061392

44. Stok C, Kok YP, van den Tempel N, van Vugt MATM. Shaping the BRCAness mutational landscape by alternative double-strand break repair, replication stress and mitotic aberrancies. Nucleic Acids Res. 2021 May 7;49(8):4239-4257. doi: 10.1093/nar/gkab151. PMID: 33744950; PMCID: PMC8096281.

45. Abou Khouzam R, Sharda M, Rao SP, Kyerewah-Kersi SM, Zeinelabdin NA, Mahmood AS, Nawafleh H, Khan MS, Venkatesh GH and Chouaib S (2023) Chronic hypoxia is associated with transcriptomic reprogramming and increased genomic instability in cancer cells. Front. Cell Dev. Biol. 11:1095419. doi: 10.3389/fcell.2023.1095419

46. Roby KF, Taylor CC, Sweetwood JP, Cheng Y, Pace JL, Tawfik O, Persons DL, Smith PG, Terranova PF. Development of a syngeneic mouse model for events related to ovarian cancer. Carcinogenesis. 2000 Apr;21(4):585-91. doi: 10.1093/carcin/21.4.585. PMID: 10753190.

47. Kelland, L. The resurgence of platinum-based cancer chemotherapy. Nat Rev Cancer 7, 573–584 (2007). https://doi.org/10.1038/nrc2167

48. Pienta KJ, Hammarlund EU, Austin RH, Axelrod R, Brown JS, Amend SR. Cancer cells employ an evolutionarily conserved polyploidization program to resist therapy. Semin Cancer Biol. 2022 Jun;81:145-159. doi: 10.1016/j.semcancer.2020.11.016. Epub 2020 Dec 1. PMID: 33276091.